

# The effect of gestational diabetes mellitus on fetal right heart growth in late-term pregnancy: A prospective study

Yuhan Wang MD<sup>1</sup> | Hongzhou Liu MD<sup>1,2</sup> | Xiaona Hu MM<sup>1</sup> | Xiaodong Hu MM<sup>1</sup> |  
 Jiamei Zhang MM<sup>3</sup> | Han Zhang MM<sup>3</sup> | Jincheng Wang MM<sup>4</sup> | Shan Su MM<sup>5</sup> |  
 Yueheng Wang MD<sup>3</sup> | Zhaohui Lyu MD<sup>1</sup>

<sup>1</sup>Department of Endocrinology, The First Medical Center, Chinese PLA General Hospital, Beijing, China

<sup>2</sup>Department of Endocrinology, First Hospital of Handan City, Handan, Hebei Province, China

<sup>3</sup>Department of Ultrasound Diagnosis, The Second Hospital of Hebei Medical University, Xinhua District, Shijiazhuang, Hebei Province, China

<sup>4</sup>Department of Radiology, Peking University Cancer Hospital, Haidian District, Beijing, China

<sup>5</sup>Department of Ultrasound, Chaoyang Hospital, Capital Medical University, Shijingshan District, Beijing, China

## Correspondence

Yueheng Wang, Department of Ultrasound, The Second Hospital of Hebei Medical University, 215 Heping Road, Shijiazhuang 050000 China.

Email: [wyhucg@sina.com](mailto:wyhucg@sina.com)

Zhaohui Lyu, Department of Endocrinology, The First Medical Center, Chinese PLA General Hospital, 28 Fuxing Road, Beijing, 100853 China.

Email: [a17531073106@163.com](mailto:a17531073106@163.com)

Yuhan Wang and Hongzhou Liu contributed equally to the article.

## Abstract

**Background:** Gestational diabetes mellitus (GDM) is a complication of pregnancy strongly associated with an increased risk of structural fetal abnormalities. As the fetal heart grows quickly during the late-term pregnancy period, it is important to understand fetal heart growth before birth. This study explored how GDM affects fetal heart growth by evaluating basic echocardiography indicators during late pregnancy.

**Methods:** This prospective, longitudinal study included 63 GDM patients (GDM group) and 67 healthy pregnant women (control group). All subjects underwent fetal echocardiography scans at gestational weeks 28–32, 32–36, and 36–40. Twelve echocardiographic indicators were assessed at each observation and analyzed by using a mixed model.

**Results:** The left atrial diameter (LA) and left ventricular end-diastolic diameter (LV) similarly increased from the first to the third observation. The right ventricular end-diastolic diameter (RV) was significantly different between the groups, and a group × time interaction was detected. The tricuspid annular peak systolic velocity (s') increased more rapidly in the GDM than the control group during the first to second observations, and the group × time interaction was significant. The increase in the tricuspid annular plane systolic excursion (TAPSE) of the GDM group was “slow-fast”, while that of the control group was “fast-slow”, during three observations. After adjusting covariates, the group difference and interaction effect of TAPSE and RV remained significant.

**Conclusions:** The differences in fetal right heart indicators between the GDM and control groups suggest that GDM may affect the structure and functional growth of the fetal right heart during late-term pregnancy.

## KEYWORDS

echocardiography, fetal heart, four-chamber view, gestational diabetes mellitus, late-term pregnancy

## 1 | BACKGROUND

Gestational diabetes mellitus (GDM) is a common complication of pregnancy that increases the risk of adverse pregnancy outcomes and has multiple adverse effects during fetal development. This metabolic disease is related to an increased rate of fetal malformations and can cause perinatal mortality.<sup>1</sup> The latest research indicates that GDM is strongly associated with an increased risk of fetal heart congenital malformations, such as fetal cardiac septal hypertrophy, ventricular wall thickening, and ventricular outflow tract obstruction.<sup>2,3</sup> A meta-analysis including 1120 GDM patients showed that GDM is associated with fetal cardiac hypertrophy, diastolic dysfunction, and overall impaired myocardial performance on fetal ultrasound.

GDM triggers insulin resistance, causing persistent intrauterine hyperglycemia that in turn impairs fetal growth. A persistent hyperglycemic state during embryonic development leads to a decrease in cardiomyocyte glycogen content and an increase in reactive oxygen species, which stimulate cardiomyocyte proliferation and hypertrophy.<sup>4</sup> Furthermore, insulin resistance is more prevalent during late-term pregnancy, as the placental secretion of anti-insulin hormones begins to increase rapidly during gestational week 28.<sup>5</sup> Thus, it is vital to observe fetal cardiac development during this period.

Fetal echocardiography is a reliable technique to assess fetal cardiac structure and function; its precision and reproducibility are widely recognized.<sup>6</sup> Basic echocardiographic indicators, such as the diameter of the fetal heart cavity, hemodynamics, and cardiac work function, are often recorded during fetal echocardiography diagnosis; obstetricians and endocrinologists can refer to these indicators as a guide for clinical practice. This study aimed to explore the effects of GDM on fetal heart growth during late-term pregnancy by prospectively evaluating the basic fetal echocardiography indicators.

## 2 | METHODS

### 2.1 | Study population

A prospective longitudinal study was conducted by the Department of Cardiac Ultrasound of the Second Hospital of Hebei Medical University between January 2020 and September 2021. In total, 71 pregnant women with GDM and 76 healthy pregnant women without diagnosing GDM were recruited to this study. This study protocol received ethical approval from the review board of Hebei Medical University. All participants and at least one family member was informed of the purpose of the study, and all participants provided written informed consent.

The subjects in both the GDM and control groups were required to meet the following inclusion criteria:  $\geq 28$  gestational weeks; singleton pregnancy; screened for diabetes mellitus at 28 weeks of gestation and underwent an oral glucose tolerance test (OGTT); and able to undergo fetal echocardiography at gestational weeks 28–32, 32–36, and 36–40. It was also a requirement that the interval between each

measurement was 4 weeks  $\pm$  5 days. The exclusion criteria were as follows: diabetes mellitus and pregnancy; other pregnancy complications, including hypertension or anemia during pregnancy, cardiovascular disease, chronic kidney disease, immune-related disease, thyroid disease, glucose corticoid or psychotropic drug use; aged  $< 18$  years; participants who did not complete the three follow-up observations, and participants with preterm delivery, termination of pregnancy, or miscarriage during the observation period. The fetal exclusion criteria were as follows: very high ( $> 4000$  g) or very low birth weight ( $< 1500$  g); twin or multiple births; and fetal malformations or chromosomal abnormalities.

Inclusion in the GDM group also required compliance with the diagnostic criteria recommended by the IADPSD<sup>7</sup>: patients with fasting blood glucose (FBG)  $\geq 5.1$  mmol/L, hPG 1 h  $\geq 10.0$  mmol/L, and hPG 2 h  $\geq 8.5$  mmol/L at 24–28 weeks of gestation were diagnosed with GDM. The study procedures were showed in Figure 1.

### 2.2 | Fetal echocardiographic measurements

Each subject has received three-time fetal echocardiographic examinations during late-term pregnancy (i.e., at gestational weeks 28–32, 32–36, and 36–40). All images were measured and saved by the Voluson E10 ultrasound machine with a probe frequency of 2–5 MHz (GE Medical Systems, Zipf, Austria). Twelve fetal echocardiography parameters were measured in this study.

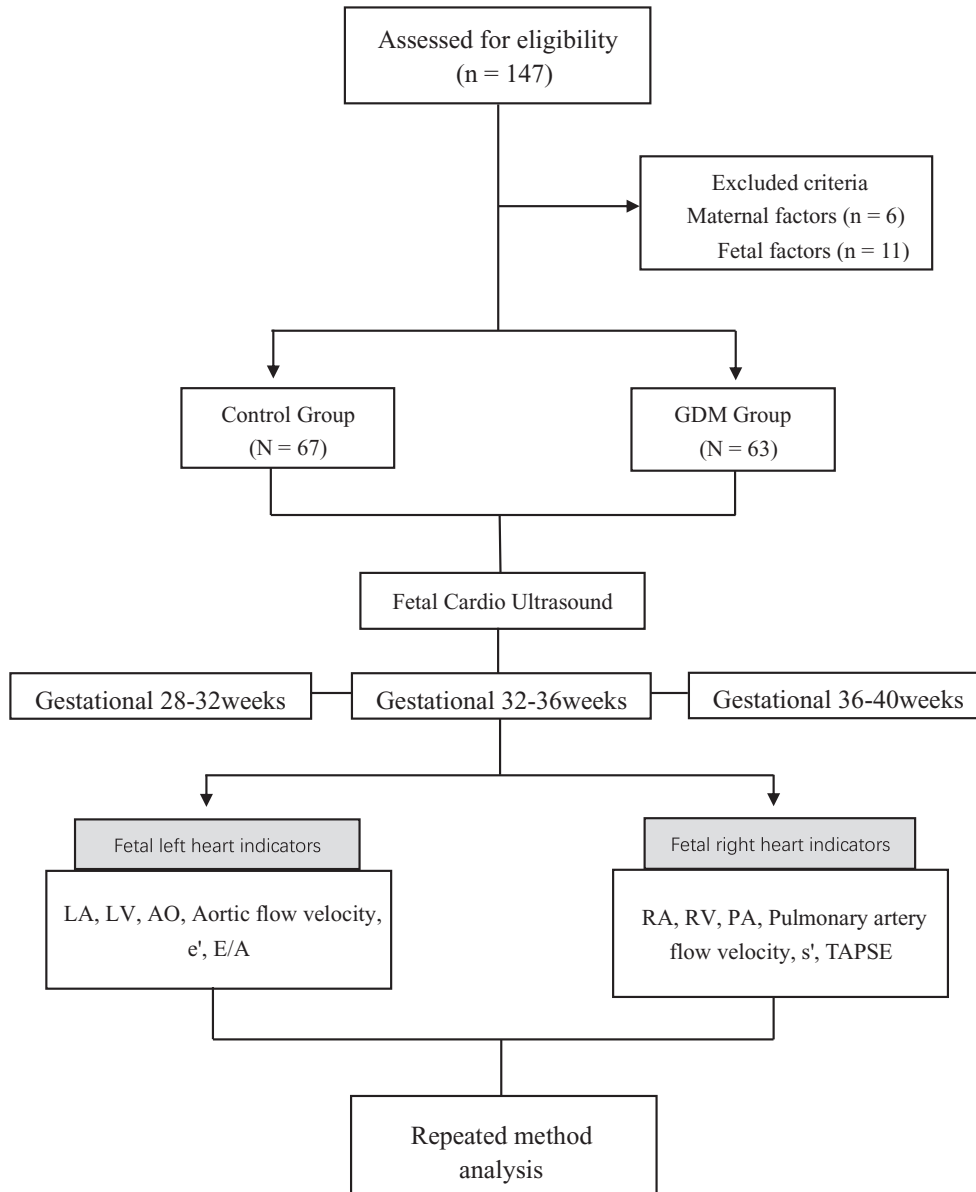
First, determining the abdominal situs and fetal position. In the normal four-chamber view (Figure 2A), the left atrial diameter (LA) and right atrial diameter (RA) were measured by calculating the length between the foramen ovale center to the inner edge of the left and right atrial lateral wall at end-systole. The left ventricular end-diastolic diameter (LV) and right ventricular end-diastolic diameter (RV) were measured by calculating the length from the septum's inner edge to the left and right ventricular lateral wall's inner edge below the annular at end-diastole.

In the longitudinal four-chamber view, the peak mitral E and A-wave velocity ratio (E/A) were measured by mitral flow pattern (Figure 3F). The pulsed tissue Doppler sample volume was placed at the annular levels to record mitral and tricuspid annular tissue Doppler spectrum to estimate the mitral annular early diastolic velocity (e') and the tricuspid annular peak systolic velocity (s') (Figure 3E).

Under the M-mode measurement, sampling at the junction of tricuspid annular and the right ventricular free wall to obtain the tricuspid annular motion curve (TAM). On the TAM curve (Figure 2D), the longitudinal displacement from the end-systolic to end-diastolic of tricuspid annular were measured to represent the tricuspid annular plane systolic excursion (TAPSE).

In the left ventricular outflow tract (LVOT) view, the aortic diameter (AO) is obtained by measuring the vertical distance between the inner edges of the aortic valve at the annular systole (Figure 2B). Obtaining the aorta spectrum to measure the aortic flow velocity.

In the right ventricular outflow tract (RVOT) view (the pulmonary artery diameter (PA) is obtained by measuring the vertical distance



**Abbreviations:** LA, left atrial diameter; LV, left ventricular end-diastolic diameter; AO, aortic diameter; e', mitral annular early diastolic velocity; E/A, peak mitral E/A-wave velocity; RA, right atrial diameter; RV, right ventricular end-diastolic diameter; PA, pulmonary artery diameter; s', tricuspid annular peak systolic velocity; TAPSE, tricuspid annular plane systolic excursion;

**FIGURE 1** Flow Chart. LA, left atrial diameter; LV, left ventricular end-diastolic diameter; AO, aortic diameter; e', mitral annular early diastolic velocity; E/A, peak mitral E/A-wave velocity; RA, right atrial diameter; RV, right ventricular end-diastolic diameter; PA, pulmonary artery diameter; s', tricuspid annular peak systolic velocity; TAPSE, tricuspid annular plane systolic excursion

between the inner edges of the pulmonary valve at the annular systole (Figure 2C). Showing the pulmonary artery spectrum to measure the pulmonary artery flow velocity.

The average of each diameter at three consecutive cardiac cycles were recorded to be analyzed in this study. The measurements were completed by a single experienced physician (JMZ) and all images were reviewed by a second physician (HZ). All the procedures were referred to the ISUOG guideline.<sup>8</sup>

### 2.3 | Statistical analysis

Baseline characteristics of the subjects were compared according to GDM status. Numerical variables are described as the mean  $\pm$  standard deviation, and categorical variables as frequencies (%). The *p*-values of the trend test comparing the GDM and control groups are reported. The *t*-test was used for analyzing numerical variables, and the Mantel-Haenszel chi-square test for analyzing categorical variables. Because

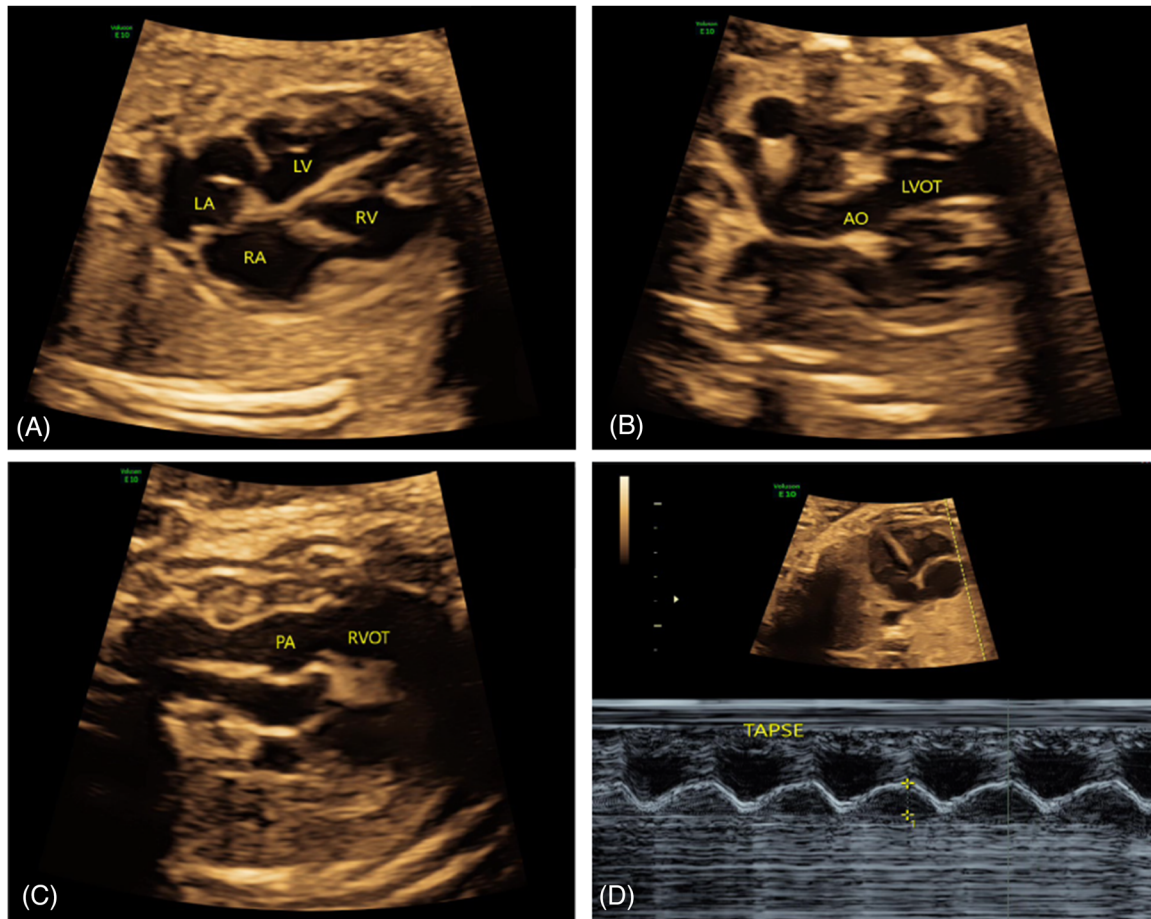


**FIGURE 2** Fetal echocardiography measurement in four-chamber and outflow tract views. Four-chamber views at 37 weeks' gestation. (A) Normal four-chamber view; (B) left ventricular outflow tract view; (C) right ventricular outflow tract view; (D) longitudinal four-chamber view. LA, left atrial diameter; LV, left ventricular end-diastolic diameter; RA, right atrial diameter; RV, right ventricular end-diastolic diameter; AO, aortic diameter; LVOT, left ventricular outflow tract; PA, pulmonary artery diameter; RVOT, right ventricular outflow tract; TAPSE, tricuspid annular plane systolic excursion

the fetal echocardiographic indicators were repeated-measures data, a multilevel model was used. We first developed a multilevel null model of the fetal echocardiographic indicators to test for differences between and within study subjects at different time points. Indicators showing significant differences between and within study subjects at the different time points were included in the actual multilevel model. Based on the similar increases in indicators between the two groups, we constructed a random intercept model with a group and the three observation time points as independent variables, fetal echocardiographic indicators as dependent variables, and subjects as a random effect to test for differences between the GDM and control groups. Then, we analyzed the group  $\times$  time interaction effects. We also developed a multilevel model adjusting for covariates. All finally analyzed patients must complete three follow-up visits, that is, there were no missing data.

We analyzed the outcomes and calculated confidence intervals using the least-squares method, and plotted the time trends to visualize group differences. The Bonferroni *t*-test was used to compare the outcome indicators at the different time points within the same sub-

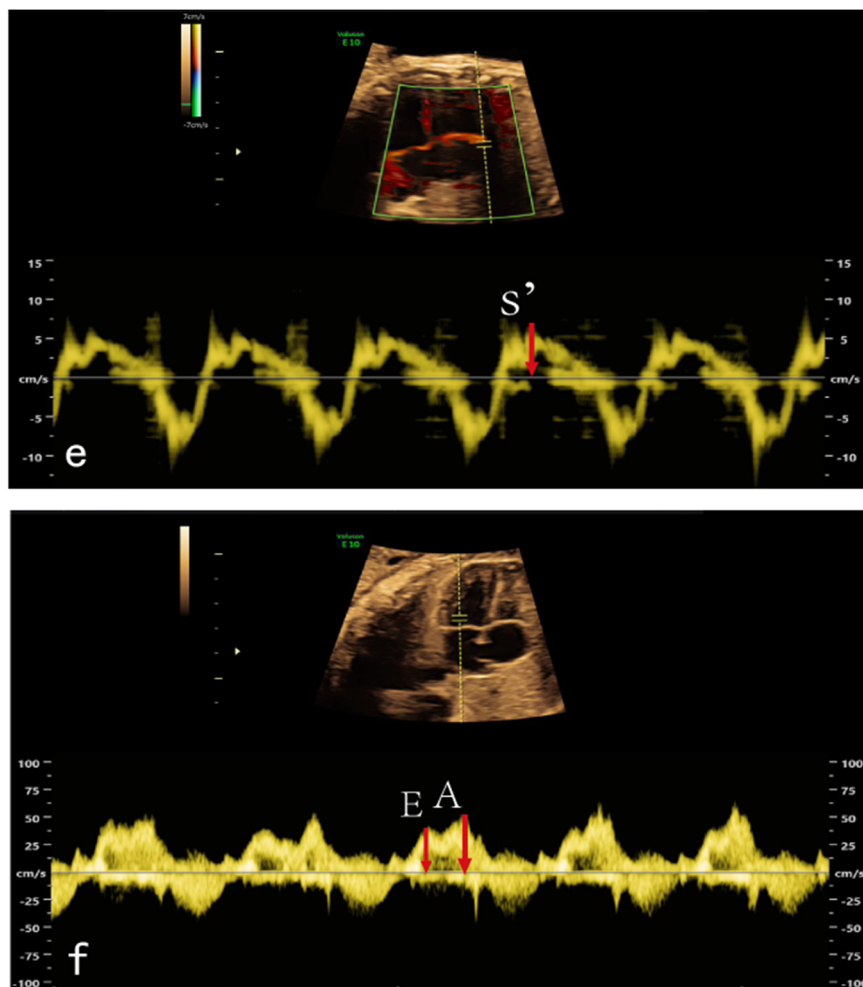
group, with an adjusted  $\alpha$  of  $.05/15 = .003$ . For the two-sided test,  $\alpha = .05$ . The statistical analysis was performed using SAS software (version 9.4; SAS Institute, Cary, NC, USA).

### 3 | RESULTS

#### 3.1 | Study population

A total of 147 participants were recruited to this study; 17 patients were excluded (6 withdrew due to preterm delivery or miscarriage, and 11 failed to complete the three follow-up visits). Table 1 shows the baseline maternal and fetal characteristics of the participants. Regarding the maternal characteristics, the GDM group had higher glycated hemoglobin (HbA1c) levels than the control group. The FBG and OGTT blood glucose levels at 1 and 2 h were significantly different from the control group. In addition, the neonatal hypoglycemia rate was higher in the GDM than control group. No differences in pregnancy age, gestational weeks at the three observation times, pre-gestational body mass

**FIGURE 3** Fetal echocardiography measurement in Doppler spectrum views. Doppler spectrum views at 37 weeks' gestation. (E) tricuspid annular tissue Doppler spectrum; (F) mitral flow pattern.  $s'$ , tricuspid annular peak systolic velocity; E, Peak mitral E-wave velocity; A, Peak mitral A-wave velocity



index (BMI), delivery mode, blood pressure, smoking history, or family history of diabetes mellitus were observed between the two groups. Also, no significant differences in fetal sex, weight, head circumference, heart rate, distress rate, or rate of admission to the neonatal intensive care unit were observed between the GDM and control groups (Table 1).

### 3.2 | Fetal left heart development

The LA and LV increased similarly between the GDM and control groups from the first to the third observation. The increases in AO during late-term pregnancy were nearly the same between the GDM and control groups, and there was no significant group  $\times$  time interaction among these three indicators (Table 2, Figure 4).

The  $e'$  increased slowly during the first to second observations in both groups, whereas it increased rapidly from the second to third time observation time point in both groups. The aortic flow velocity increased during late-term pregnancy in the GDM and control groups. In addition, the increase in E/A ratio reflected the increase in left heart work in both groups (Table 2, Figure 4). The multilevel model adjusting for covariates showed a similar trend as null model in left heart indicators (Table S4, Figure S6).

### 3.3 | Fetal right heart development

RA increased rapidly in the GDM and control groups from the first to second observations, but the rate of increase slowed from the second to the third observations. The increase in PA detected in the GDM group was nearly the same as that in the control group, from the first to the second observation time point; however, the increase in the GDM group was slightly faster than that in the control group between the second and third observations. No significant group  $\times$  time interaction was detected between RA and PA. However, the RV was significantly different between the groups, and the group  $\times$  time interaction was significant. The RV level in the GDM group was higher than that in the control group from the first observation onward. As the pregnancies continued, the increase of RV in the GDM group was greater than that in the control group, and the difference in RV between the two groups gradually became larger during the three observation periods (Table 2, Figure 5).

The increase in  $s'$  was significantly different between the GDM and control groups during late-term pregnancy. A significant group  $\times$  time interaction was observed. First, the estimated  $s'$  in the control group was higher than in the GDM group at the first observation. As  $s'$  was increasing more rapidly in the GDM than the control group, the graphs of  $s'$  crossed between the first and second observations, and

**TABLE 1** Baseline characteristic

	GDM N = 63	CG N = 67	X <sup>2</sup> /t	p
Maternal characteristic				
Age (year)	29.58 ± 2.87	29.79 ± 2.63	.42	.67
Gestational weeks (weeks ± days)				
First observation	28 ± 3.83	28 ± 3.84	.04	.97
Second observation	34 ± 4.00	34 ± 4.15	.65	.51
Third observation	38 ± 4.02	38 ± 4.01	−.003	.98
Delivery mode (%)				
Vaginal delivery	34 (50.7)	35 (55.6)	.11	.74
Cesarean-section	33 (49.3)	28 (44.4)		
Primipara (%)	38 (56.7)	37 (58.7)	.09	.76
Pre-gestational BMI (kg/m <sup>2</sup> )	22.02 ± 3.22	22.40 ± 4.17	.56	.57
HbA1c (%)	5.75 ± .20	4.92 ± .63	−10.37	<.001
OGTT (mmol/L)				
FBG	5.39 ± .46	5.11 ± .37	−3.75	<.001
1 h	10.02 ± .87	9.36 ± .75	−4.61	<.001
2 h	8.07 ± .84	7.59 ± .61	−3.68	<.001
Blood pressure (mmHg)				
SBP	117.07 ± 9.6	116.64 ± 9.27	−2.64	.79
DBP	71.90 ± 8.39	73.00 ± 8.25	.75	.46
Smoke history (%)	4 (6)	5 (7.9)	.20	.66
Diabetes mellitus family history (%)	12 (19.0)	13 (19.4)	.003	.96
Fetal characteristic				
Fetal sex (%)				
Male	31 (49.2)	32 (46.3)	.11	.74
Female	32 (50.8)	36 (53.7)		
Weight (g)	3430 ± 447	3447 ± 254	−2.71	.79
Head circumference (cm)	33.52 ± .53	33.43 ± .54	1.01	.31
Apgar Score (5 min)	8.65 ± .60	8.63 ± .62	.22	.82
Fetal distress (%)	2 (3.2)	1 (1.5)	1.26	.53
Neonatal random blood glucose (mmol/L)	4.48 ± .36	4.52 ± .31	−.59	.56
Heart rate (per min)	143.7 ± 4.9	142.7 ± 4.8	1.17	.25
Neonatal hypoglycemia (%)	3 (4.8)	1 (1.5)	1.16	.28
Admission to neonatal intensive care unit (%)	5 (79.4)	5 (74.6)	.10	.92

**Abbreviation:** CG, Control Group. FBG, Fasting blood glucose.

Values are expressed as means ± SD (standard variation) or frequency (%).

the estimated  $s'$  in the GDM group became higher than in the control group. The pulmonary artery flow velocity showed a similar increasing trend during the three observations, but no significant group × time interaction was detected (Table 2, Figure 5).

TAPSE reflects the work of the fetal right heart. The increases in TAPSE values of the two groups diverged during late-term pregnancy. The TAPSE value in the GDM group was lower than in the control group at the first observation. The increases in the two groups then diverged between the first and second observations. The increase by the GDM

group was “slow-fast”, indicating that the rate of increase in the GDM group was slower than in the control group from the first to the second observation, but had increased by the third observation. However, the control group showed the opposite pattern; the increase was “fast-slow”. The TAPSE value in the GDM group was always lower than in the control group during late-term pregnancy (Table 2, Figure 5). The multilevel model adjusting for covariates showed the similar trend as null model in right heart indicators (Table S4, Figure S7).

**TABLE 2** Mixed model for fetal echocardiographic indicators

	28–32 weeks			32–36 weeks			36–40 weeks			p-value				
	GDM	CG	95% CI	GDM	CG	95% CI	GDM	CG	95% CI	Trend		Group difference		
										Model 1	Model 2	Model 1	Model 2	Interaction
AO	4.15 (3.97,4.32)	4.03 (3.87,4.21)	(6.44,6.78)	6.61 (6.44,6.78)	6.37 (6.20,6.53)	(7.32,7.58)	7.45 (7.32,7.58)	7.24 (7.11,7.36)	(7.11,7.36)	<.001	<.001	<.001	<.001	.57
AO flow velocity	76.95 (76.33,77.57)	76.53 (75.36,76.57)	(80.46,81.66)	82.63 (82.01,83.25)	81.06 (80.46,81.66)	(84.73,85.97)	85.34 (84.73,85.97)	84.30 (83.69,84.90)	(83.69,84.90)	<.001	<.001	<.001	<.001	.45
e'	3.08 (2.99,3.18)	3.01 (2.92,3.10)	(3.62,3.80)	3.82 (3.73,3.91)	3.71 (3.62,3.80)	(5.77,5.95)	5.86 (5.77,5.95)	5.68 (5.60,5.77)	(5.60,5.77)	<.001	<.001	<.001	<.001	.48
LA	8.73 (8.51,8.95)	8.92 (8.71,9.13)	(10.94,11.37)	11.16 (10.94,11.37)	11.27 (11.06,11.48)	(13.19,13.62)	13.40 (13.19,13.62)	13.48 (13.27,13.69)	(13.27,13.69)	.01	.01	.26	.26	.80
LV	8.97 (8.63,9.32)	8.69 (8.35,9.3)	(13.15,13.85)	13.50 (13.15,13.85)	12.98 (12.65,13.32)	(15.78,16.45)	16.11 (15.78,16.45)	15.58 (15.26,15.91)	(15.26,15.91)	<.001	<.001	.02	.02	.60
E/A	.66 (.65,.68)	.68 (.67,.69)	(.74,.77)	.75 (.74,.76)	.76 (.74,.77)	(.80,.83)	.82 (.80,.83)	.83 (.81,.84)	(.81,.84)	<.001	<.001	.51	.51	.78
PA	5.00 (4.90,5.10)	5.08 (4.98,5.18)	(7.62,7.82)	7.72 (7.62,7.82)	7.79 (7.69,7.89)	(8.00,8.20)	8.10 (8.00,8.20)	8.05 (7.96,8.15)	(7.96,8.15)	<.001	<.001	.54	.54	.31
PA flow velocity	65.65 (64.73,66.57)	64.48 (63.58,65.37)	(69.05,70.90)	69.97 (69.05,70.90)	68.69 (67.79,69.58)	(76.32,78.16)	77.24 (76.32,78.16)	75.42 (74.52,76.31)	(74.52,76.31)	<.001	<.001	.005	.005	.48
s'	3.79 (3.64,3.94)	4.00 (3.85,4.14)	(4.88,5.17)	5.03 (4.88,5.17)	4.79 (4.65,4.93)	(6.75,7.00)	6.88 (6.75,7.00)	6.42 (6.30,6.54)	(6.30,6.54)	<.001	<.001	.01	.01	<.001
RA	9.43 (9.11,9.76)	9.29 (8.97,9.61)	(13.36,13.99)	13.67 (13.36,13.99)	14.04 (13.73,14.36)	(14.21,14.86)	14.53 (14.21,14.86)	14.02 (13.70,14.35)	(13.70,14.35)	<.001	<.001	.04	.04	.48
RV	9.62 (9.33,9.90)	9.02 (8.74,9.30)	(13.72,14.30)	14.00 (13.72,14.30)	13.19 (12.91,13.46)	(16.71,17.29)	17.00 (16.71,17.29)	15.43 (15.16,15.71)	(15.16,15.71)	<.001	<.001	<.001	<.001	<.001
TAPSE	6.66 (6.54,6.79)	7.16 (7.05,7.28)	(7.47,7.25)	7.60 (7.47,7.25)	8.67 (8.54,8.78)	(9.04,9.29)	9.17 (9.04,9.29)	9.47 (9.35,9.59)	(9.35,9.59)	<.001	<.001	<.001	<.001	<.001

Abbreviations: AO flow velocity, aortic flow velocity; AO, aortic diameter; e', mitral annular early diastolic velocity; E/A, peak mitral E/A-wave velocity; LA, left atrial diameter; LV, left ventricular end-diastolic diameter; PA flow velocity, pulmonary artery flow velocity; PA, pulmonary artery diameter; RA, right atrial diameter; RV, right ventricular end-diastolic diameter; s', tricuspid annular peak systolic velocity; TAPSE, tricuspid annular plane systolic excursion.

All values are expressed as means  $\pm$  95% CI (confidence interval).

Fetal left heart echocardiographic indicator.

Fetal right heart echocardiographic indicator.

Model 1: Mixed model with random effect.

Model 2: Mixed model with time and group interaction.

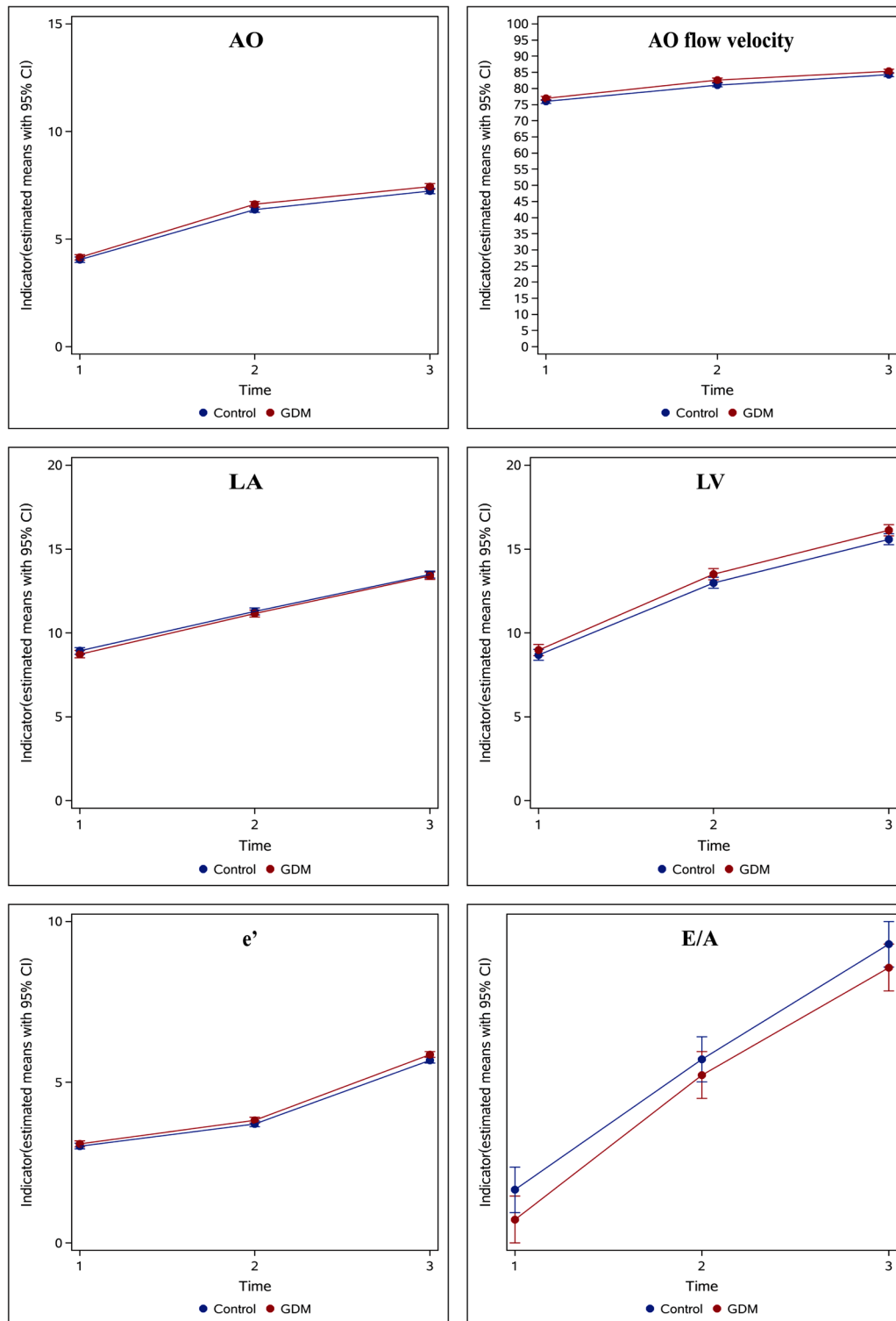


**FIGURE 4** Group plot of left heart indicators. Estimated means with 95% CIs from mixed models for left heart echocardiographic indicators at three observations (Time1: 28–32 weeks' gestation, Time2: 32–36 weeks' gestation, Time3: 36–40 weeks' gestation) in GDM and control group. LA, left atrial diameter; LV, left ventricular end-diastolic diameter; AO, aortic diameter; AO flow velocity, aortic flow velocity; e', mitral annular early diastolic velocity; E/A, peak mitral E/A-wave velocity



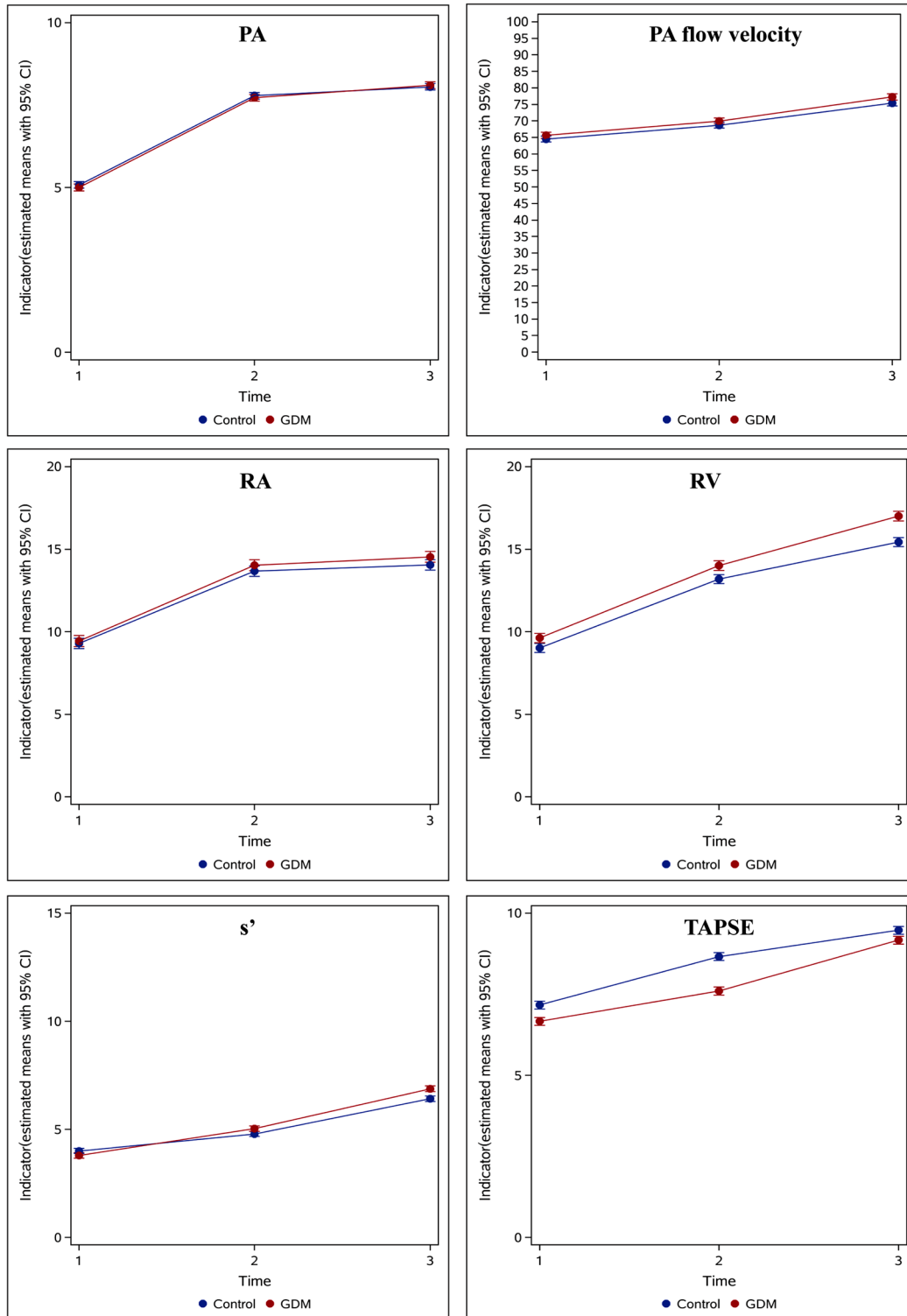


**FIGURE 5** Group plot of right heart indicators. Estimated means with 95% CIs from mixed models for right heart echocardiographic indicators at three observations (Time1: 28–32 weeks' gestation, Time2: 32–36 weeks' gestation, Time3: 36–40 weeks' gestation) in GDM and control group. RA, right atrial diameter; RV, right ventricular end-diastolic diameter; PA, pulmonary artery diameter; PA flow velocity, pulmonary artery blood flow velocity; s', tricuspid annular peak systolic velocity; TAPSE, tricuspid annular plane systolic excursion

Tables S3.1 and S3.2 shows the contribution of the covariates included in the mixed model to each indicator. Several of the covariates contributed significantly ( $p < .05$ ). Pre-pregnancy BMI contributed to LA and  $e'$  ( $p = .02$  and  $.04$ , respectively), and HbA1c contributed to aortic flow velocity and RA (both  $p = .04$ ). A maternal family history of diabetes mellitus contributed to  $e'$  ( $p = .03$ ). Fetal weight contributed to RA and RV ( $p = .02$  and  $.002$ , respectively), and fetal head circumference contributed to  $e'$  ( $p = .02$ ). Figure 2 shows the outcomes of all indicators after adjusting for related covariates, including the age of the pregnancies, HbA1c level, pre-pregnancy BMI, blood pressure, history of diabetes mellitus, smoking history, and fetal weight, head circumference, sex, and distress (Tables S3.1–S3.2).

## 4 | DISCUSSION

Pregnancy is a complex physiological process. The fetus exchanges many substances with its mother via the placenta, so metabolic abnormalities of the mother directly affect the metabolic environment of the fetus.<sup>9</sup> Gestational diabetes mellitus (GDM) provides an unfavorable “high glucose” intrauterine environment due to insulin resistance. This process may persist throughout fetal growth.<sup>10,11</sup> Previous studies have shown that GDM is related to excessive fetal myocardial growth, which leads to interventricular septal thickening<sup>12,13</sup> and thus may impair fetal heart development.

In our study, no significant group with time interaction was detected for the fetal left heart indicators, the growing trend in left cardiac structural and functional indicators were also similar between the GDM and control groups. In our results, the peak mitral E and A-wave velocity ratio ratio (E/A) and aortic flow velocity were not significantly different between the GDM and control groups during late-term pregnancy. Ren et al. similarly reported that GDM did not affect the E/A ratio during gestational weeks 27–31.<sup>14</sup> In addition, a meta-analysis including 1120 GDM patients at about 30 gestational weeks reported no difference in the E/A ratio or left heart myocardial performance index between normal and GDM pregnancies.<sup>15</sup> These evidences suggesting that the effect of GDM on fetal left heart may not strongly emerge at late-term pregnancy.

The right ventricle is dominant in the fetal circulation which may be affected earlier than the left ventricle, as it is more sensitive to load changes in fetal growth.<sup>16,17</sup> In our study, the growing trend of right ventricular end-diastolic diameter (RV) in the GDM group became higher than that in the control group, and the difference in two groups became larger in the whole observation period. The rapid increase of RV in GDM group may affect the entire cardiac structure of the fetal myocardium and increase the spherical index,<sup>18–20</sup> which may be a sign of reduced myocardial compliance.

Another significant difference between our GDM and control groups was the tricuspid annular plane systolic excursion (TAPSE), which represents the working function of the right heart. Different patterns in the increase of TAPSE were observed in two groups. Interestingly, the GDM group showed a slow-fast increase, whereas the control group exhibited a fast-slow trend in observation period.

This demonstrates that right ventricular working function in GDM group performed a different growing trend at this stage. Compared to another similar recent study, Yovera and her colleagues found that the fetus' TAPSE level in GDM subjects was significantly lower than uncomplicated pregnancies at gestational 32–40 weeks.<sup>21</sup> The delay of lung maturity may explain this phenomenon. As the lung maturity of GDM fetus occurs later than the normal fetus on the 28–34 weeks, the fetal right ventricle working function may be influenced simultaneously.<sup>22,23</sup> This could lead to heart remodeling continuing into adulthood, and increased susceptibility to adult diseases.<sup>24</sup>

The tricuspid annular peak systolic velocity ( $s'$ ) is an indicator of systolic right ventricular function. The  $s'$  value was slightly lower in our GDM group than the control group at the first observation (28–32 weeks of gestation), suggesting a hemodynamic difference between the two groups. However, as the pregnancies progressed, the increase became more rapid and the  $s'$  value was slightly higher in the GDM than control group at 36–40 gestational weeks. This observation suggests that the hemodynamics changed in the GDM group during late-term pregnancy. Chu et al. detected significantly higher pulmonary velocity in their GDM group fetus compared to the control group in the first two trimesters of pregnancy, and in the last trimester of pregnancy there was no significant difference between the groups.<sup>25</sup> We speculated that the change in hemodynamics seen in the GDM group was a compensatory response to the reduction in function at 28–32 weeks of gestation. This reflected the fetal heart appears to be a highly flexible, responsive, and adaptive structure.

We identified some factors in the covariate-adjusted mixed model that were associated with fetal echocardiographic indicators such as pre-pregnancy BMI, the HbA1c level, a family history of diabetes mellitus, fetal weight, and head circumference. These metabolic indicators were also proved to be associated with structural growth to the myocardium in offspring.<sup>15,26,27</sup> Our longitudinal analysis of the fetal echocardiographic parameters showed that GDM may affect fetal heart growth during late-term pregnancy compared to healthy control pregnancies. Particularly, we observed significant differences in right heart indicators, such as the RV, TAPSE, and  $s'$ . These results suggest that GDM may have a profound impact on the development of the fetal right heart during late-term pregnancy, which is consistent with the findings of recent clinical studies.<sup>22,28</sup>

## 5 | LIMITATIONS

Several limitations of our study should be mentioned. Because our study aimed to elucidate the association between GDM and fetal cardiac development, we did not perform a subgroup analysis according to the treatment style of GDM subjects, whereas studies have shown that glycemic control levels of GDM patients is associated with fetal myocardial development.<sup>29,30</sup> In addition, our study observed fetal heart development during late pregnancy; long term evaluation is still needed to demonstrate the potential effect of GDM on offspring's cardio development.

## 6 | CONCLUSION

The increase in fetal echocardiographic indicators in the left heart was similar between our GDM and control groups, suggesting that GDM may not affect left heart development during late-term pregnancy. However, the increases in several fetal right heart indicators were significantly greater in the GDM group, suggesting that GDM affects fetal right heart structural and functional growth during late-term pregnancy.

## ACKNOWLEDGMENT

Not applicable.

## CONFLICT OF INTEREST

None of the authors have any competing interests in relation to this study. This study was not supported by any organization. All authors have read and approved the submitted version of the manuscript.

## REFERENCES

- Ornoy A, Becker M, Weinstein-Fudim L, Ergaz Z. Diabetes during pregnancy: a maternal disease complicating the course of pregnancy with long-term deleterious effects on the offspring: a clinical review. *Int J Mol Sci.* 2021;22(6):2965.
- Papazoglou AS, Moysidis DV, Panagopoulos P, et al. Maternal diabetes mellitus and its impact on the risk of delivering a child with congenital heart disease: a systematic review and meta-analysis. *J Matern Fetal Neonatal Med.* 2021;1-10.
- Bhorat I, Pillay M, Reddy T. Determination of the fetal myocardial performance index in women with gestational impaired glucose tolerance and to assess whether this parameter is a possible prognostic indicator of adverse fetal outcome. *J Matern Fetal Neonatal Med.* 2018;31(15):2019-2026.
- Jin YM, Zhao SZ, Zhang ZL, et al. High glucose level induces cardiovascular dysplasia during early embryo development. *Exp Clin Endocrinol Diabetes.* 2013;121(8):448-454.
- de Gennaro G, Palla G, Battini L, et al. The role of adipokines in the pathogenesis of gestational diabetes mellitus. *Gynecol Endocrinol.* 2019;35(9):737-751.
- McBrien A, Hornberger LK. Early fetal echocardiography. *Birth Defects Res.* 2019;111(8):370-379.
- Weinert LS, International association of diabetes and pregnancy study groups recommendations on the diagnosis and classification of hyperglycemia in pregnancy: comment to the international association of diabetes and pregnancy study groups consensus panel. *Diabetes Care.* 2010;33(7): e97; author reply e98.
- Carvalho JS, Allan LD, Chaoui R, et al. International society of ultrasound in obstetrics and gynecology, ISUOG practice guidelines (updated): sonographic screening examination of the fetal heart. *Ultrasound Obstet Gynecol.* 2013;41(3):348-359.
- Mirabelli M, Chiefari E, Tocci V, Greco E, Foti D, Brunetti A. Gestational diabetes: implications for fetal growth, intervention timing, and treatment options. *Curr Opin Pharmacol.* 2021;1-10.
- Kua KL, Hu S, Wang C, et al. Fetal hyperglycemia acutely induces persistent insulin resistance in skeletal muscle. *J Endocrinol.* 2019;242(1):M1-M15.
- Silva L, Plösch T, Toledo F, Faas MM, Sobrevia L. Adenosine kinase and cardiovascular fetal programming in gestational diabetes mellitus. *Biochim Biophys Acta Mol Basis Dis.* 2020;1866(2):165397.
- HePing ZhangYuqi, LuYu XuHuiying. Correlation between fetal cardiac function and interventricular septal thickness in fetuses of diabetic mothers. *Chinese J Med Imag.* 2013;21(10):771-774. 779.
- Fouda UM, Abou El Kassem M, Hefny SM, Fouda RM, Hashem AT. Role of fetal echocardiography in the evaluation of structure and function of fetal heart in diabetic pregnancies. *J Matern Fetal Neonatal Med.* 2013;26:571-575.
- Ren Y, Zhou Q, Yan Y, Chu C, Gui Y, Li X. Characterization of fetal cardiac structure and function detected by echocardiography in women with normal pregnancy and gestational diabetes mellitus. 2011:459-465.
- Depla AL, De Wit L, Steenhuis TJ, et al. Effect of maternal diabetes on fetal heart function on echocardiography: systematic review and meta-analysis. *Ultrasound Obstet Gynecol.* 2021;57(4):539-550.
- Faber JW, Hagoort J, Moorman AFM, Christoffels VM, Jensen B. Quantified growth of the human embryonic heart. *Biol Open.* 2021;10(2). bio057059.
- Gardiner HM. Response of the fetal heart to changes in load: from hyperplasia to heart failure. *Heart.* 2005;91(7):871-873.
- Turgut E, Turan G, Özdemir H, Aktulum F, Bayram M, Karcaaltincaba D. Fetal cardiac morphology and geometry in pregnancies with class A1 and A2 gestational diabetes mellitus. *J Matern Fetal Neonatal Med.* 2022;35(6):1023-1027.
- Wang D, Liu C, Liu X, Zhang Y, Wang Y. Evaluation of prenatal changes in fetal cardiac morphology and function in maternal diabetes mellitus using a novel fetal speckle-tracking analysis: a prospective cohort study. *Cardiovasc Ultrasound.* 2021;19(1):25.
- Luo Y, Xiao F, Long C, et al. Evaluation of the sphericity index of the fetal heart during middle and late pregnancy using fetal HQ. *J Matern Fetal Neonatal Med.* 2021:1-6.
- Yovera L, Zaharia M, Jachymski T, et al. Impact of gestational diabetes mellitus on fetal cardiac morphology and function: cohort comparison of second- and third-trimester fetuses. *Ultrasound Obstet Gynecol.* 2021;57(4):607-613.
- López Sánchez F, Delgado Sánchez E, Duyos Mateo I, González Álvarez MC, Antolín Alvarado E, Bartha JL. Evaluation of fetal lung maturity by quantitative analysis (quantusflm) in women with gestational diabetes mellitus. *Fetal Diagn Ther.* 2019;45(5):345-352.
- Kjos SL, Berkowitz KM, Kung B. Prospective delivery of reliably dated term infants of diabetic mothers without determination of fetal lung maturity: comparison to historical control. *J Matern Fetal Neonatal Med.* 2002;12(6):433-437.
- Crispi F, Crovetto F, Rodríguez-López M, Á Sepúlveda-Martínez, Miranda J, Gratacós E. Postnatal persistence of cardiac remodeling and dysfunction in late fetal growth restriction. *Minerva Obstet Gynecol.* 2021;73(4):471.
- Chu C, Gui YH, Ren YY, Shi LY. The impacts of maternal gestational diabetes mellitus (GDM) on fetal hearts. *Biomed Environ Sci.* 2012;25(1):15-22.
- Boney CM, Verma A, Tucker R, Vohr BR. Metabolic syndrome in childhood: association with birth weight, maternal obesity, and gestational diabetes mellitus. *Pediatrics.* 2005;115(3):e290-6.
- Cade WT, Levy PT, Tinius RA, et al. Markers of maternal and infant metabolism are associated with ventricular dysfunction in infants of obese women with type 2 diabetes. *Pediatr Res.* 2017;82(5): 768-775.
- Jatavan P, Lerthirawong T, Sekararithi R, et al. The correlation of fetal cardiac function with gestational diabetes mellitus (GDM) and oxidative stress levels. *J Perinat Med.* 2020;48(5):471-476.
- Özalp M, Demir O, Dinç G, et al. Fetal cardiac Doppler changes in gestational diabetic pregnancies and its relationship with perinatal outcomes. *J Obstet Gynaecol Res.* 2021;47(10):3480-3487.

30. Borat I, Pillay M, Reddy T. Assessment of the fetal myocardial performance index in well-controlled gestational diabetics and to determine whether it is predictive of adverse perinatal outcome. *Pediatr Cardiol*. 2019;40(7):1460-1467.

#### SUPPORTING INFORMATION

Additional supporting information can be found online in the Supporting Information section at the end of this article.

**How to cite this article:** Wang Y, Liu H, Hu X, et al. The effect of gestational diabetes mellitus on fetal right heart growth in late-term pregnancy: A prospective study. *Echocardiography*. 2022;39:1101-1112. <https://doi.org/10.1111/echo.15425>